2003

Generation–recombination noise in gallium nitride-based quantum well structures

Rolando S. Duran
Florida International University

Grover L. Larkins Jr.
Florida International University

Carolyn M. Van Vliet
University of Miami

Hadis Morkoç
Virginia Commonwealth University

Generation–recombination noise in gallium nitride-based quantum well structures

Rolando S. Duran and Grover L. Larkins, Jr.
Center for Engineering and Applied Sciences, Florida International University, Miami, Florida 33199

Carolyne M. Van Vliet[a)]
Department of Physics, University of Miami, Coral Gables, Florida 33124

Hadis Morkoç
Department of Electrical Engineering, Virginia Commonwealth University, Richmond, Virginia 23284

(Received 1 August 2002; accepted 29 January 2003)

Electronic noise has been investigated in $Al_xGa_{1-x}N/GaN$ modulation-doped field-effect transistors of submicron dimensions, grown by molecular beam epitaxy techniques. Some 20 devices were grown on a sapphire substrate. Conduction takes place in the quasi-two-dimensional (2D) layer of the junction (*xy* plane) which is perpendicular to the triangular quantum well (*z* direction). A nondoped intrinsic buffer layer separates the Si-doped donors in the $Al_xGa_{1-x}N$ layer from the 2D transistor plane. Since all contacts must reach through the $Al_xGa_{1-x}N$ layer to connect internally to the 2D plane, parallel conduction through this layer is a feature of all modulation-doped devices. The excess noise has been analyzed as a sum of Lorentzian spectra and $1/f^{\alpha}$ noise. The Lorentzian noise is ascribed to trapping of the carriers in the $Al_xGa_{1-x}N$ layer. The trap depths have been obtained from Arrhenius plots of $\log(\tau T^2)$ versus $1000/T$. Comparison with previous noise results for GaAs devices shows that: (a) many more trapping levels are present in these nitride-based devices and (b) the traps are deeper (farther below the conduction band) than for GaAs, as expected for higher band-gap materials. Furthermore, the magnitude of the noise is strongly dependent on the level of depletion of the $Al_xGa_{1-x}N$ donor layer. We also note that the trap-measured energies are in good agreement with the energies obtained by deep level transient spectroscopy. © *2003 American Institute of Physics.* [DOI: 10.1063/1.1562000]

I. INTRODUCTION AND PREVIOUS WORK

Gated and nongated modulation-doped field-effect transistors (MODFETs), based on $Al_xGa_{1-x}As/GaAs$ heterojunctions, were studied in the Electrical Noise Research Laboratory of Florida International University (FIU) by Chen *et al.* The results of her study are laid down in her dissertation (FIU 1998) and in various subsequently published articles.[1,2] At present much interest continues in nitride-based devices, see, e.g., the recent international symposium on nitride devices, reported in Ref. 3. These materials provide for high temperature-resistant devices, since their band gaps are considerably higher than that of the GaAs-type devices. Like GaAs, the band gap of GaN is direct, thus enabling the fabrication of blue light emitting diodes and lasers in conjunction with metal-semiconductor field-effect transistors (MESFETs) or MODFETs. Also, nitride-based devices are very promising for high power applications (see a recent survey article in Spectrum, Ref. 4). The material properties are presently well understood.[5–14] In heterojunctions of $Al_xGa_{1-x}N/GaN$ a quasitriangular quantum well is formed at the interface due to the conduction-band offset of the two constituents. At room temperature the following phenomenological expression for the dependence of the band gap on the aluminum molar fraction x has been reported:[15,16] $E_g(x) = 3.42 + 1.35x + 0.99x^2$ (eV) for $0 \leqslant x \leqslant 0.65$. Thus, for $x = 0.3$, the band gap difference is $\cong 0.5$ eV, of which about 0.35 eV contributes to the conduction band offset. When the doping of the $Al_xGa_{1-x}N$ is known, the occupancies of the discrete quantum well levels near the Fermi level and resulting sheet carrier density of the interface can be fairly well computed (see, e.g., Shur's book).[17] For a donor doping of $10^{17}-10^{18}$ cm^{-3}, sheet densities of $10^{12}-10^{13}$ cm^{-2} are commonly obtained and also measured from the Hall-effect data. The main technological problem is the absence of a near-lattice matched substrate since bulk GaN had not yet been produced at the time of our studies. Sapphire or SiC substrates were employed instead. Since the conduction plane of MODFETs is parallel to the substrate junction and electrically insulated from it, this has no adverse noise effects according to the present study. Very recently[18] researchers from Japan Sumitomo's GaN Substrate Program have been using a process called hydride vapor-phase epitaxy in which they start by growing a thick film of GaN on a substrate of gallium arsenide. Afterwards they cut the substrate, remove it, lap, and polish the circle of GaN to turn it into substrate itself.

So far, noise studies on modulation-doped heterostructures of $Al_xGa_{1-x}N/GaN$ have been rather rare. Garrido *et al.*[19] report only $1/f$ noise, attributed to the internal source and drain contacts; the reported Hooge parameter is $\alpha_H = 5$

[a)]Author to whom correspondence should be addressed; electronic mail: vanvliet@physics.miami.edu

$\times 10^{-4}$. Balandin[20] has observed typical $1/f$ noise, plus some generation-recombination noise ($g-r$ noise) ''bumps,'' with trapping time constants of 0.1 ms and 16 μs. The $1/f$ noise is attributed to surface traps, whereas the bulk traps responsible for the $g-r$ noise were not identified, since only room temperature data are reported. More complete data are given by Rumyantsev *et al.*.[21,22] Again, there is much $1/f$ noise, which is fitted by Hooge's formula, yielding a Hooge parameter of $10^{-1}-10^{-4}$. From the $g-r$ noise, a discrete trapping level is found at 0.42 eV below the conduction band.

Furthermore, a number of articles dealing with low frequency noise in molecular beam epitaxial (MBE) grown GaN layers have been published by Leung *et al.*[23] and Levinshtein *et al.*;[24] also results on MESFETs and MOSFETs, based on GaN have been reported by Rumyantsev *et al.*[25] However, all these reported data are not about noise in MODFETs and are very restricted, since the frequency limit of 100 kHz is due to the exclusive use of a fast fourier transform (FFT) analyzer instead of regular analog heterodyned wave analyzers which can go up to several hundred megahertz. Secondly, the $1/f$ noise is dominant in all studies and detailed temperature dependent data are near absent, whereas the physical origin of the noise remains mostly obscure. On the contrary, in the present study we report noise spectra from 1 Hz to 10 MHz, using a HP3589A wave analyzer, which was used in the FFT mode from 1 Hz to 40 kHz and in the analog mode from 40 kHz to 10 MHz (the analyzer is capable of going to 150 MHz, but generally the ''excess noise'' (over and above thermal noise) is too small to be observed beyond 10 MHz). The temperature was varied from 325 to 78 K, using a Janis liquid N_2 bath cryostat and an autotuning thermal controller, LakeShore Temperature Controller Model 330, LakeShore Cryotronics Co. Preliminary results of this research were presented and discussed by one of the authors (Duran[26]).

This article is further structured as follows. In Sec. II we describe the layout of the MBE samples used for this study, grown at Virginia Commonwealth University. In Sec. III we briefly discuss some specifics of the measurement procedure. Then, in Sec. IV we present the main aspect of this article: detailed measurements of the current spectral density $S_i(f)$ of two samples over the full frequency range 1 Hz–10 MHz, temperature dependence, and the resulting Arrhenius plots of the observed Lorentzians. Finally, some theoretical concepts of $g-r$ trapping noise, interpretation, and possible physical origin of the noise are discussed in Secs. V and VI.

II. THE DEVICES

The sample used consists of an array of many $Al_xGa_{1-x}N$/GaN MODFETs on a single GaN-based chip, mounted in an outer frame of the bonding pads. This outer frame was attached only for mechanical stability during transportation. Each device has a rectangular pattern (see Fig. 1) with two symmetric contact pads on each side of the ''width.'' Both of them are drains. Only one of these drains is bonded to a wire. The two contact pads on each side of the ''length'' are the gate and the source. Four of these devices have three wires bonded to a gold overlayer to establish contacts to drain, the source, and the gate, respectively. The other end of each wire is connected to a metallic stripe, to which minicoaxial cables were bonded; these cables go to the port connectors of the cryostat. Some preparatory work was done before using the sample properly. The metallic frame (square) was cut off so that each ''ray '' was electrically insulated, in order to establish the required connections.

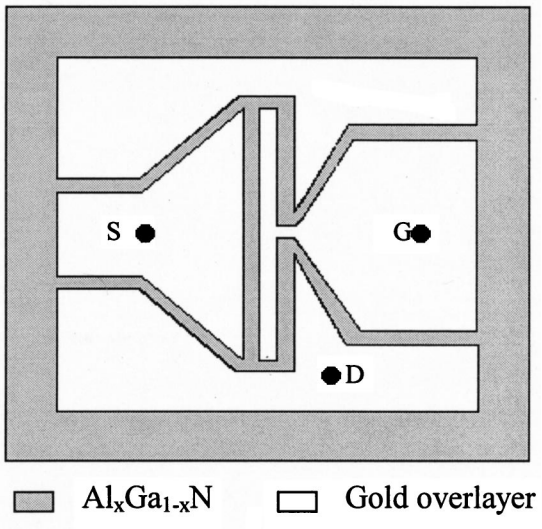

FIG. 1. Top view of the device.

The leads to one separate device as observed under a microscope with a 250× magnification, are shown in Fig. 1. The gate ''length'' L is about 1 μm by design and the ''width'' is either 40, 80, or 150 μm in different columns. These distances were estimated under the microscope. In the present bonding configuration, only half of the drain ''width'' is effective. Vertically, each device has the standard MODFET layer structure. The doped $Al_xGa_{1-x}N$ layer was separated from the junction with a nondoped 3 nm spacer, deposited on unintentionally doped GaN, grown on the *c* plane of sapphire substrates. The samples were, in many respects, similar as described in a recent study, which gives details of the growth technique.[27]

III. MEASUREMENT PROCEDURE

The device under test (DUT) was mounted against the cold finger of the liquid N_2 bath cryostat. The leads from the sample were connected via 1 mm minicoaxial cables to the ports of the cryostat and from there via regular coax cables to a brass box containing the input circuitry, which was similar as for previous measurements on gallium arsenide-based MODFETs. The DUT was generally operated in the linear range of the I_D versus V_{DS} curve, with the gate voltage V_{GS} equal to zero, or a fixed negative voltage (sample ND-101), or with the gate potential floating (sample ND-102). The drain current was controlled by a precision ten-turn helipot across noise-free 12 V batteries, with the DUT resistance in series with a wirewound 20 kΩ load resistor R_L, which was ac grounded via a 10 μF capacitor and 100 pF ''bleeder.'' For calibration we used a white spectrum noise generator (Quan-Tech 420B till 100 kHz, avalanche diode source for

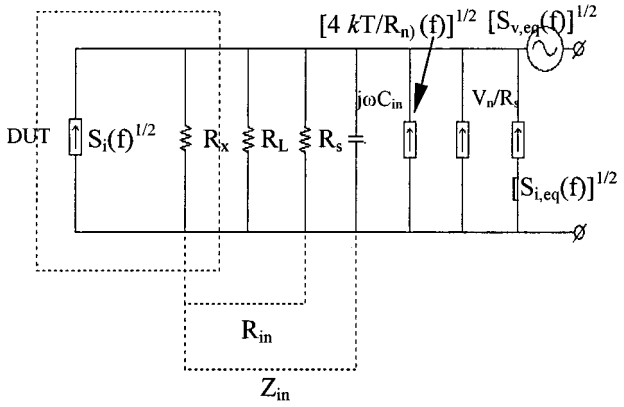

FIG. 2. Equivalent scheme of the experimental setup.

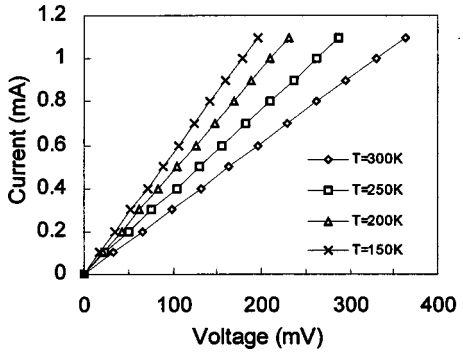

FIG. 3. $I-V$ characteristics: ND-101. $V_{GS}=0$ V.

100 kHz to 10 MHz) which was connected to a 20 Ω resistor in series with a large (20 kΩ) resistor R_S, thus providing a Norton generator current source $\nu_N/(R_S+20)\approx\nu_N/R_S$. The actual circuit is given in Refs. 1 and 2, while the equivalent circuit, including the voltage noise ($S_{v,\mathrm{eq}}$) and current noise ($S_{I,\mathrm{eq}}$) of the low noise Brookdeal 5184 (Princeton Applied Research) preamplifier, is given in Fig. 2. Note that, except for the voltage source of the preamplifier $[(S_{v,\mathrm{eq}})]^{1/2}\approx(0.8\ \mathrm{nV}/\sqrt{\mathrm{Hz}})$, all noise sources are given as current sources, the relevant noise source being $[S_i(f)]^{1/2}$ (Norton generator representing the excess noise of the DUT) $[4kT/R_{\mathrm{in}}]^{1/2}$ (Norton generator representing the Johnson noise of the input resistance, $R_{\mathrm{in}}=R_x(\mathrm{DUT})\|R_L\|R_S$), and $[S_{i,\mathrm{eq}}]^{1/2}$ (Norton generator representing the preamplifier).

Whereas most investigators usually measure the voltage noise $S_v(f)$ of the sample, using the output dB readings of their FFT analyzers directly, this method is fallacious if one goes to higher frequencies with an analog wave analyzer, since the shunting effect of the input capacitance—particularly serious if connections via coaxial cables to a cryostat must be made—plays an important role. Therefore, we have consistently employed a measurement of the current noise $S_i(f)$ via the "three-point measurement method" which is trouble free for linear devices up to very high frequencies (for nonlinear devices a four-point method must be used, which will not be discussed here; see e.g., Ref. 28).

Thus, let M_1 be the output analyzer reading with a current flowing through the DUT and the noise generator turned off; M_2 be the output analyzer reading with the noise-calibration source applied to the terminals without current flowing through the DUT and the noise generator set to a value ν_n; and M_3 be the output analyzer reading without current flowing through the DUT and the noise generator off. Then, we have, with all readings reduced to a bandwidth $\Delta f=1$ Hz, and with $Z_{\mathrm{in}}=R_{\mathrm{in}}\|1/j\omega C_{\mathrm{in}}=R_{\mathrm{in}}/(1+j\omega C_{\mathrm{in}}R_{\mathrm{in}})$

$$M_1=X\left\{|Z_{\mathrm{in}}|^2\left[S_{i,\mathrm{DUT}}(f)+\frac{4kT}{R_{\mathrm{in}}}+S_{i,\mathrm{eq}}(f)\right]+S_{v,\mathrm{eq}}\right\},\qquad(1)$$

where X is a constant resulting from the amplification and averaging of the analog or FFT detector of the system. Further,

$$M_2=X\left\{|Z_{\mathrm{in}}|^2\left[\frac{S_{v,\mathrm{ng}}(f)}{R_S^2}+\frac{4kT}{R_{\mathrm{in}}}+S_{i,\mathrm{eq}}(f)\right]+S_{v,\mathrm{eq}}\right\},\qquad(2)$$

where $S_{v,\mathrm{ng}}\equiv(\nu_n)^2$ is the voltage intensity output of the calibration noise generator in a bandwidth of 1 Hz. Finally,

$$M_3=X\left\{|Z_{\mathrm{in}}|^2\left[\frac{4kT}{R_{\mathrm{in}}}+S_{i,\mathrm{eq}}(f)\right]+S_{v,\mathrm{eq}}\right\}.\qquad(3)$$

With little algebra it follows that

$$S_{i,\mathrm{DUT}}(f)=\frac{M_1-M_3}{M_2-M_3}\frac{S_{v,\mathrm{ng}}}{R_S^2}.\qquad(4)$$

Note that $S_{i,\mathrm{DUT}}(f)$ includes only *excess noise*, i.e., noise over and above the thermal noise, since the thermal noise of the DUT is comprised in $4kT/R_{\mathrm{in}}$. Whereas Z_{in} may involve a *RC* rolloff due to the parasitic input capacitance C_{in}, the resulting current noise spectrum $S_{i,\mathrm{DUT}}$, as obtained from Eq. (4), is not affected by this rolloff, since $|Z_i|^2$ drops out of the result. For this reason the measurements could be continued to ~10 MHz, above which frequency the excess noise generally disappeared in the Johnson noise. An increase in current would allow us to go to higher frequencies, but in most cases we approached the breakdown field, $E=3\times10^6$ V/m in GaN. (So, with a channel length of ~1 μm, the constraint is $V_{\mathrm{DS}}<3$ V; to stay in the linear region of the I_D versus V_{DS} characteristic, we restricted ourselves to $V_{\mathrm{DS}}\leqslant0.5$ V.)

IV. MEASUREMENT RESULTS

A. Data for device ND-101

1. Current–voltage ($I-V$) characteristics

Figure 3 shows the $I-V$ characteristics for sample ND-101 with $V_{\mathrm{GS}}=0$ V. Data are given for different temperatures: $T=300$, 250, 200, and 150 K. In the range $V_{\mathrm{DS}}\leqslant500$ mV, the device behaved linearly. From these data we determined $I(T)$ for $V=200$ mV. Clearly, this function is proportional to the two-dimensional (2D) conductance $G_{2\mathrm{D}}(T)$ of the channel, which in turn is proportional to the conductivity σ, since

$$G_{2\mathrm{D}}=\sigma\frac{w}{L_{\mathrm{ch}}},\qquad(5)$$

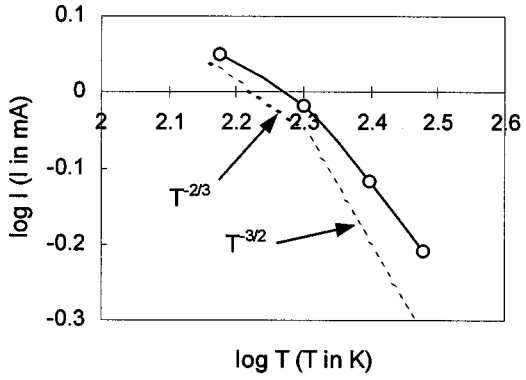

FIG. 4. Conductance (relative units) vs temperature: ND-101.

where w is the channel ''width'' and L_{ch} is the channel ''length'' (approximately twice the gate length L; see Fig. 1). Therefore, the plot of $I(T)$ for V fixed at 200 mV represents $\sigma(T)$ for the device. We assume that the donors are all ionized for the entire temperature range, i.e., $n_0 = N_D \lambda_c$, λ_c being a characteristic length.[17] Hence

$$\sigma(T) \approx q \mu_n(T) N_D \lambda_c . \tag{6}$$

Thus, the plot of $I(T)$, given in Fig. 4, represents the temperature dependence of the electron mobility $\mu_n(T)$. We notice that $\mu_n(T)$ decreases with T. For temperatures $\geqslant 200$ K, the curve approaches the theoretical value for lattice scattering associated with polar optical phonons, $\sigma \propto T^{3/2}$.[29] Finally, we notice that the curve for $\mu_n(T)$ is very similar to the corresponding curve for GaAs,[2] but shifted to higher temperatures, as one would expect for this higher band-gap material.

2. Noise data with $V_{GS}=0$ at room temperature ($T=295$ K)

Figure 5 shows the data in the range 1 Hz–3 MHz for zero gate-source voltage at room temperature. At first glance the points—without the solid drawn line—look roughly as

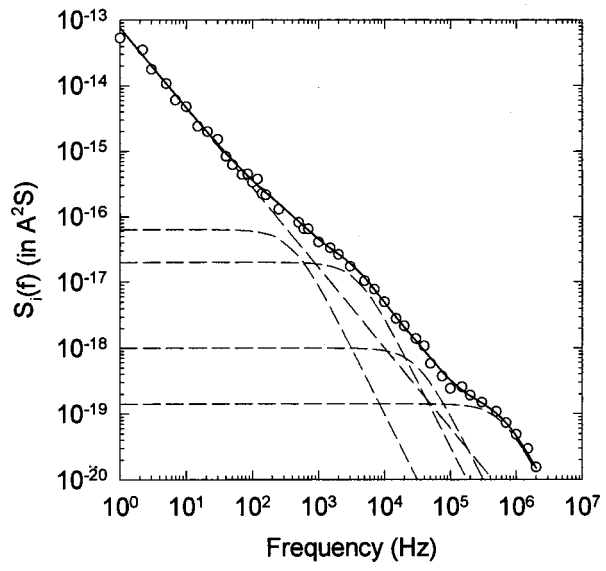

FIG. 5. Noise spectrum and decomposition: ND-101, $T=295$ K.

TABLE I. Values of the parameters A_i and τ_i for sample ND-101, $T=295$ K.

i	$\log(A_i)$ (dB)	τ_I (s)
1	−162.0	4.0×10^{-4}
2	−167.0	4.0×10^{-5}
3	−180.0	5.0×10^{-6}
4	−188.5	2.5×10^{-7}

''$1/f$'' noise. However, the reader will note that we present well-averaged point-by-point data whose accuracy was determined to be within 5%. Such data are far more meaningful than the usual ''fuzzy lines'' obtained from nonpost averaged FFT measurements of noise spectra, encountered in much of the present-day literature [see e.g., the nitride-based high electron mobility transistors spectra by Rumyantsev *et al.*].[21] We therefore set out to fit the results by the most accurate decomposition

$$S_i(\omega) = B\left(\frac{2\pi}{\omega}\right)^{\alpha} + \sum_i \frac{A_i}{1+\omega^2\tau_i^2} \tag{7}$$

representing $1/f$-like noise plus a sum of Lorentzians. Fitting was done with a least square deviation GRAPH-PAD PRISM software program (cf. Ref. 30) or with Microsoft EXCEL. The decomposition so obtained is shown in dashed lines. Four Lorentzians are clearly discernible, while the $1/f$-like noise follows accurately from the low frequency data (1–100 Hz) with exponent $\alpha = 1.22$. A summary of the constants B, α, (A_i, τ_i) with $i=1,...,4$ is given in Table 1. When the five parts of the spectrum are added we obtain the full-drawn fluid line; clearly the fit of the experimental points is very good.

3. Noise spectra with $V_{GS}=0$ at cryogenic temperatures

Below room temperature noise spectra were obtained at 250, 200, 150, 120, 100, 84, and 78.5 K. The $1/f$-like noise for these temperatures was negligible in this sample. Four to six Lorentzians are discernible in the spectra. We give the results only for $T=250$ and 84 K, displayed in Figs. 6 and 7, respectively. In all figures the open circles represent the measured point-by-point spectra. The dashed lines represent the decomposition in $1/f^{\alpha}$ and $\{L_i\}$, $i=1,...,$ maximum 6; the solid line is the sum of the various parts, giving the most accurate fit to the measured points, an exception being at the highest frequencies where the differences $M_1 - M_3$ were small. Basically, the presented analyses are accurate and realistic.[31] The various Lorentzian time constants τ are listed in Table II.

4. Arrhenius plots

According to the theory (see next section), the time constants should vary with temperature according to

$$\tau_i \propto T^{-2} \exp[(\varepsilon_c - \varepsilon_i)/kT], \tag{8}$$

where ε_c is the bottom of the conduction band and ε_i is the trap-level energy. We have therefore plotted $\log(\tau_i T^2)$ versus $1000/T$ in Fig. 8. The data are taken from Table II. Each

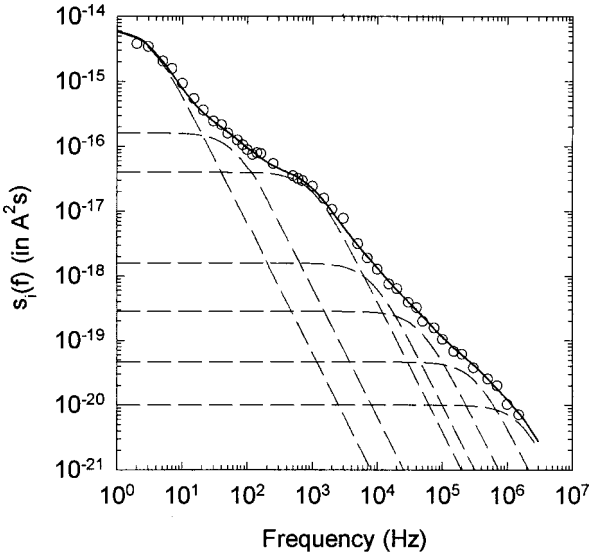

FIG. 6. Noise spectrum and decomposition: ND-101, $T=250$ K.

point in the temperature verticals corresponds to a row in Table II. A judicious analysis allows us to group the points on the plot as belonging to straight lines. Thus, nine Arrhenius curves could be constructed with the slopes successively becoming weaker, indicative of shallower traps, as the temperature decreases ($1000/T$ increases).

5. Spectra for $V_{GS}\neq 0$

Measurements were made for $V_{GS}=-2$ V, and for $V_{GS}=-6$ V, at $T=250$ and 120 K. The spectra for $V_{GS}=-2$ V were not noticeably different from those for $V_{GS}=0$ V. In the $V_{GS}=-6$ V curves the Lorentzian structure has largely disappeared, (see Fig. 9) with $1/f$-like noise now being dominant. This behavior is similar as observed for arsenide-based devices.[2] It is attributed to the smaller conductivity of the $Al_xGa_{1-x}N$ layer, due to increased depletion under large negative gate bias. We also looked at the spectra for $V_{GS}=+2$ V. These spectra show 4–6 Lorentzians and

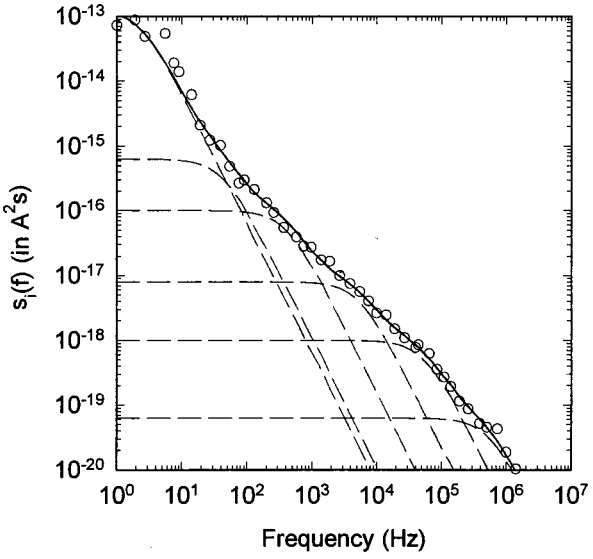

FIG. 7. Noise spectrum and decomposition: ND-101, $T=84$ K.

TABLE II. Values of the parameters A_i and τ_i for sample ND-101 [Eq. (7)].

	$T=295$ K		$T=250$ K		$T=200$ K		$T=150$ K		$T=120$ K		$T=100$ K		$T=84$ K		$T=78$ K	
i	$\log(A_i)$	τ_I	$\log(A_i)$	τ_I	$\log(A_i)$	τ_I	$\log(A_i)$	τ_I	$\log(A_i)$	τ_I	$\log(A_i)$	τ_I	$\log(A_i)$	τ_I	$\log(A_i)$	τ_I
1	−132.0	1.0×10^{-1}	−142.0	1.0×10^{-2}	−138.0	1.3×10^{-2}	−133.4	1.5×10^{-2}	−121.0	1.6×10^{-1}	−135.0	5.0×10^{-2}	−129.0	7.0×10^{-2}	−137.8	2.7×10^{-2}
2	−143.0	2.6×10^{-2}	−157.9	2.5×10^{-3}	−143.0	4.8×10^{-3}	−146.0	4.5×10^{-4}	−166.0	7.0×10^{-5}	−177.0	8.5×10^{-6}	−152.0	3.8×10^{-3}	−167.0	1.5×10^{-4}
3	−147.5	6.7×10^{-3}	−165.0	2.7×10^{-4}	−149.2	7.2×10^{-4}	−164.2	1.2×10^{-4}	−181.0	4.4×10^{-6}	−197.0	3.5×10^{-7}	−160.0	4.0×10^{-4}	−180.0	3.2×10^{-6}
4	−157.2	1.0×10^{-3}	−172.7	2.0×10^{-5}	−167.2	2.9×10^{-5}	−175.6	6.0×10^{-7}	−191.0	8.0×10^{-8}	…	…	−171.0	3.0×10^{-5}	−200.0	9.0×10^{-8}
5	−162.3	1.8×10^{-4}	−185.0	3.6×10^{-6}	−170.8	9.7×10^{-6}	−189.9	4.5×10^{-7}	…	…	…	…	−180.0	3.0×10^{-6}	…	…
6	−169.4	4.0×10^{-5}	−193.0	5.0×10^{-7}	−184.0	8.0×10^{-7}	…	…	…	…	…	…	−192.0	3.0×10^{-7}	…	…
7	−176.0	7.0×10^{-6}	…	…	…	…	…	…	…	…	…	…	…	…	…	…
8	−177.0	2.6×10^{-7}	…	…	…	…	…	…	…	…	…	…	…	…	…	…

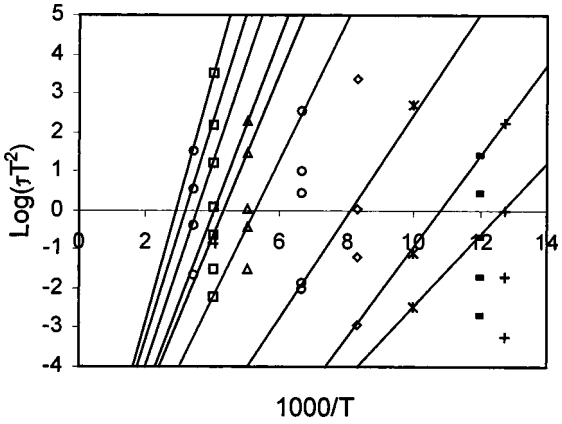

FIG. 8. Arrhenius plot: ND-101, $V_{GS}=0$ V.

differ little in structure from those for $V_{GS}=0$ V. The magnitude of the noise increased, however, by about 30 dB.

B. Data for device ND-102

For this device no gate lead was connected. In this way, the gate voltage will float to a spontaneous value according to the steady-state condition of the whole device. We obtained the $I-V$ characteristics, which were linear up to $V_{GS}=0.5$ V. For larger drain voltage the onset of saturation started to show up. The noise spectra were measured for $T=325$, 295, 250, 200, 150, 100, and 80 K. The Lorentzians for this sample were generally fewer and more pronounced. Figure 10 gives the spectrum for $T=250$ K, decomposed as $1/f$ noise plus two Lorentzians.

V. ELEMENTS OF TRAPPING GENERATION-RECOMBINATION NOISE ANALYSIS

The theory of multiple trapping noise in homogeneous materials (no band bending, horizontal bands only) has been presented in essence at a variety of places. Summary versions of the theory have been given in Appendix A of Ref. 2

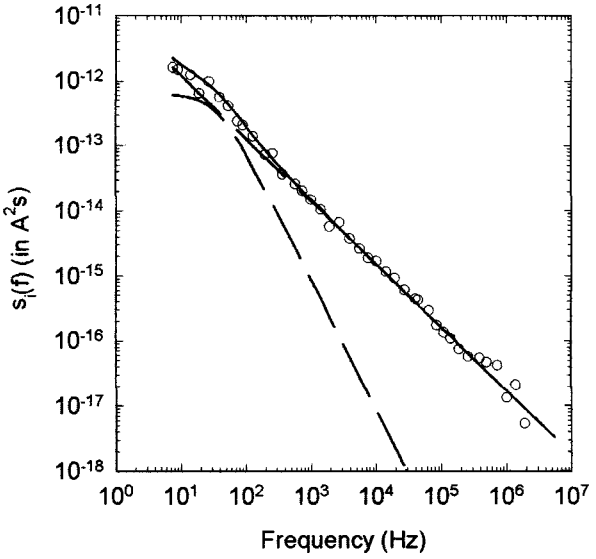

FIG. 9. Noise spectrum and decomposition: ND-101, $T=120$ K, $V_{GS}=-6$ V.

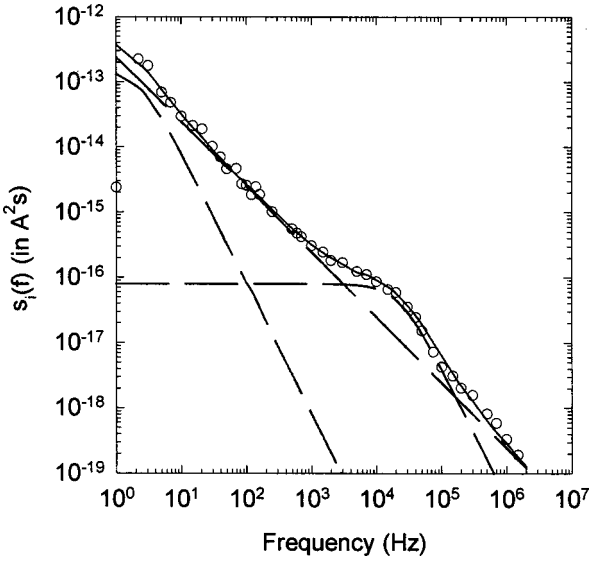

FIG. 10. Noise spectrum and decomposition: ND-102, floating V_{GS}, $T=250$ K.

and at the 16th International Conference on Noise and Fluctuations in Gainesville, Florida, 2001.[32] A fuller account is being published elsewhere.[33] Basically, the theory shows the same features as the single trap theory, given previously by Van Rheenen *et al.*[34] and by Copeland.[35]

One considers a nondegenerate conduction band with carrier density $n\equiv n_s$ in equilibrium with $s-1$ trapping levels of occupancy n_i and abundance N_i. Because of charge neutrality, $\Delta n=-\Sigma_{i=1}^{s-1}\Delta n_i$; we thus have a $(s-1)$ variate Markov process; the stochastic variable can be represented by the vector $\mathbf{a}(t)=\{n_1(t),\ldots,n_{s-1}(t)\}$. The conditional probability $P(\mathbf{a},t|\mathbf{a}',0)$ then satisfies the master equation (ME)

$$\frac{\partial P(\mathbf{a},t|\mathbf{a}',0)}{\partial t}=\sum_{\mathbf{a}''}\left[P(\mathbf{a}'',t|\mathbf{a}',0)W(\mathbf{a}'',\mathbf{a})-P(\mathbf{a},t|\mathbf{a}'',0)W(\mathbf{a},\mathbf{a}'')\right], \tag{9}$$

where $W(\mathbf{a}'',\mathbf{a})$ is the transition rate per second in an interval $\Delta t\to 0$, as obtainable from Fermi's golden rule. Thus these rates contain the cross sections for the transitions (see the next paragraph).

The ME Eq. (6.3) is seldom solvable, nor need it be, for most pertinent noise information is obtained from the first two moment equations for the conditional averages $\langle\ldots.\rangle_a$ [i.e., the averages in the subensemble with fixed initial conditions, $|\mathbf{a}'0)$]; they read

$$\frac{\partial}{\partial t}\langle\mathbf{a}(t)\rangle_{\mathbf{a}'}=\langle\mathbf{A}[\mathbf{a}(t)]\rangle_{\mathbf{a}'} \tag{10}$$

and

$$\frac{\partial}{\partial t}\langle\mathbf{a}(t)\mathbf{a}(t)\rangle_{\mathbf{a}'}=\langle\mathbf{aA}[\mathbf{a}(t)]\rangle_{\mathbf{a}'}+\langle\mathbf{A}[\mathbf{a}(t)]\rangle_{\mathbf{a}'}+\langle\mathbf{B}[\mathbf{a}(t)]\rangle_{\mathbf{a}'}, \tag{11}$$

where $\mathbf{A}$ is the vector comprising the first-order Fokker–Planck (FP) moments and $\mathbf{B}$ is the dyad comprising the

second-order Fokker–Planck moments. Though cloaked in the general language of Brownian motion phenomena, the ''phenomenological equation'' Eq. (10) turns out to yield the ordinary carrier kinetic equations (Shockley equations), while Eq. (11) yields the strength of the fluctuations, variances, and covariances, as first obtained in the ''multivariate $g-r$ theorem'' by Van Vliet and Blok. Carrying the general formulation only one step further, we note that a first order Taylor expansion around equilibrium, i.e.,

$$\mathbf{A}[\mathbf{a}(t)]=\mathbf{A}(\mathbf{a}_0)-\mathbf{M}\Delta\mathbf{a}(t) \tag{12}$$

leads for Eq. (10) to $s-1$ linearized regression equations

$$\frac{\partial\langle\Delta\mathbf{a}(t)\rangle_{\mathbf{a}'}}{\partial t}=-\mathbf{M}\langle\Delta\mathbf{a}(t)\rangle_{\mathbf{a}'}, \tag{13}$$

where $\mathbf{M}$ is the phenomenological relaxation matrix with elements

$$M_{ij}=-\partial A_i(\mathbf{a}_0)/\partial a_j, \quad (i,j=1...s-1), \tag{14}$$

while Eq. (12) for the stationary state $\partial/\partial t=0$ leads to

$$\langle\Delta\mathbf{a}\Delta\mathbf{a}\rangle\mathbf{M}^{\mathrm{tr}}+\mathbf{M}\langle\Delta\mathbf{a}\Delta\mathbf{a}\rangle=\mathbf{B}(\mathbf{a}_0). \tag{15}$$

In thermal equilibrium both terms on the left hand side are equal and we have the explicit result for the variance-covariance dyad

$$\langle\Delta\mathbf{a}\Delta\mathbf{a}\rangle=-\tfrac{1}{2}\mathbf{M}^{-1}\mathbf{B}(\mathbf{a}_0), \tag{16}$$

where $\mathbf{M}^{-1}$ is the reciprocal of $\mathbf{M}$. Equations (13)–(16) are the main results.

We now return to the specific $g-r$ theory and the trapping problem. The first-order FP moments were found to be[36,37]

$$A_i=\sum_{k=1}^{s}{}' \,[p_{ki}(n_1\cdots n_s)-p_{ik}(n_1\cdots n_s)](i=1...s-1), \tag{17}$$

where the prime as usual indicates that $k=i$ is to be omitted. Note that we included the extraneous variable $n_s\equiv n$ in the population vector $\mathbf{a}=(n_1\ldots n_s)$. The p_{ki} are the transition rates from ''level'' k to ''level'' i. In view of our assumption that each trapping level only interacts with the conduction band we have

$$p_{ij}(n_1\cdots n_s)=0 \ \text{ unless } \ i=s \ \text{ or } \ j=s. \tag{18}$$

Moreover, using quasibimolecular generation and recombination rates we write

$$p_{is}=\alpha n_i\equiv\delta_i n_{\mathrm{SR}i}n_i, \tag{19}$$

$$p_{si}=\delta_i n(N_i-n_i); \tag{20}$$

the second equality in Eq. (19) defines the Shockley–Read ''would-be'' occupancies: it is the number of carriers that would be in the conduction band *if* the Fermi level would coincide with the trap level ε_i and the spin-valley degeneracy factor g_i were unity. This follows from *detailed balance*,

$$n_{\mathrm{SR}i}n_{i0}=n_0(N_i-n_{i0}) \tag{21}$$

and Fermi statistics for the trap

$$n_{i0}/N_i=\frac{1}{1+g_i\exp[(\varepsilon_i-\varepsilon_F)/kT]} \tag{22}$$

so that by simple algebra

$$n_{\mathrm{SR}i}=n_0g_i\exp\left(\frac{\varepsilon_i-\varepsilon_F}{kT}\right)=n_0\exp\left(\frac{\varepsilon_i+kT\ln g_i-\varepsilon_F}{kT}\right). \tag{23}$$

Further, from Eqs. (14), (17), and (18) and noting from the constraint that $\partial/\partial n_k$ involves terms $(\partial/\partial n)(dn/dn_k)=-\partial/\partial n$ $(k=1,...s-1)$, we obtain

$$M_{ii}=\delta_i(n_0+n_{\mathrm{SR}i}+N_i-n_{i0}), \tag{24}$$

$$M_{ij}=\delta_i(N_i-n_{i0}), i\neq j. \tag{25}$$

Furthermore, writing $\delta_i=\sigma_i\langle\nu_n\rangle$ where σ_i is the cross section for electron capture and $\langle\nu_n\rangle$ is the average free electron velocity, we obtain

$$\left.\begin{aligned}M_{ii}&=\langle\nu_n\rangle\sigma_i(n_{\mathrm{SR}i}+n_0+N_i-n_{i0})\\ M_{ij}&=\langle\nu_n\rangle\sigma_i(N_i-n_{i0}) \quad (i\neq j)\end{aligned}\right\}. \tag{26}$$

If, in addition, the traps are not too numerous we can, with Van Rheenen *et al.*,[34] neglect the terms N_i-n_{i0} in M_{ii}, as for their single trap case. Clearly, then, we find for the $(s-1)$ eigenvalues of the secular equation $|M_{ij}-\delta_{ij}(1/\tau_i)|=0$ the result

$$\frac{1}{\tau_i}=\langle\nu_n\rangle\sigma_i(n_{\mathrm{SR}i}+n_0)\approx\langle\nu_n\rangle\sigma_iN_cg_i\exp[(\varepsilon_i-\varepsilon_c)/kT], \tag{27}$$

where we assumed temperatures $>T_{\min}$ for which $n_{\mathrm{SR}i}=n_0$, and where $N_c=2(2\pi m_n^*kT/h^2)^{3/2}$ is the statistical weight of the conduction band. We note that $\langle\nu_n\rangle\propto T^{1/2}$. Thus, Arrhenius plots of $\log(\tau_iT^2)$ versus $1/T$ yield the trap depths $(\varepsilon_c-\varepsilon_i)$, as announced in Sec. IV.

In order to find the complete spectra we must now evaluate the covariances Eq. (16) which requires the second-order Fokker–Planck moments. Without further details we state here the Copeland-like results[35]

$$\langle\Delta n_i^2\rangle=N_i\frac{g_i\exp[(\varepsilon_i-\varepsilon_F)/kT]}{\{1+g_i\exp[(\varepsilon_i-\varepsilon_F)/kT]\}^2}=\frac{N_i}{\left[\exp\left(\frac{\gamma_i}{2}\right)+\exp\left(-\frac{\gamma_i}{2}\right)\right]^2}, \tag{28}$$

where

$$\gamma_i\equiv(\varepsilon_i-\varepsilon_F)/kT+\ln g_i. \tag{29}$$

Basically, we have an inverted $\cosh^2$ dependence, which for the spectra this leads to

$$S_{\Delta n}(\omega)=4\sum_{i=1}^{s-1}N_i\tau_i\frac{\{1/4\,\mathrm{sech}^2[\gamma_i(\varepsilon_F)/2]\}}{1+\omega^2\tau_i^2} \tag{30}$$

with $\gamma(\varepsilon_F)$ given by Eq. (29). For the current noise we then obtain

$$S_i(\omega)=4\frac{I_0^2}{n_0^2}\sum_{i=1}^{s-1}N_i\tau_i\frac{\{1/4\,\mathrm{sech}^2[\gamma_i(\varepsilon_F)/2]\}}{1+\omega^2\tau_i^2}. \tag{31}$$

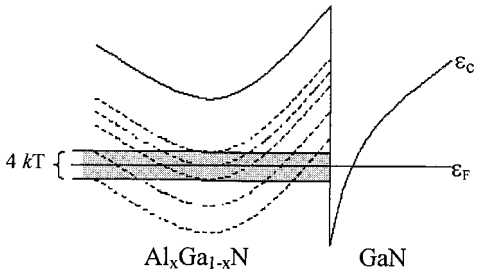

FIG. 11. Band diagram of $Al_xGa_{1-x}N$/GaN heterojuncture with traps.

We now discuss the reduction factor {...} in Eqs. (30) and (31). From Eq. (28) we see that this factor is alternatively written as

$$1/4\,\mathrm{sech}^2(\gamma_i(\varepsilon_F)/2) = \frac{g_i \exp[(\varepsilon_i-\varepsilon_F)/kT]}{\{1+g_i \exp[(\varepsilon_i-\varepsilon_F)/kT]\}^2} = f_i(1-f_i), \tag{32}$$

where in accordance with Eq. (22) f is the average occupancy factor of the traps, i.e., the (modified) Fermi function

$$f_i = \frac{1}{g_i \exp[(\varepsilon_i-\varepsilon_F)/kT]+1}, \tag{33}$$

$$1-f_i = \frac{1}{g_i^{-1} \exp[(\varepsilon_F-\varepsilon_i)/kT]+1}. \tag{34}$$

The reduction factor $f_i(1-f_i)$ causes only traps near the Fermi level (an interval $\varepsilon_F \pm 2kT$) to be selected. Therefore, in *homogeneous* materials, one observes seldom more than two to three Lorentzians, and the envelope spectrum is never $1/f$-like over more than 2 decades.

However, for materials with band bending, such as occur in MODFETs, the distance to the quasi-Fermi level is variable, as can be seen from the standard band picture (see Fig. 11). Therefore, a large range of traps can contribute to the noise. This is reflected in our measured spectra which contain up to six Lorentzians at a given temperature, visible over a frequency range of 6 decades. The modifications of the above theory for space-charge layers are presented in the recent version,[33] which affirms the conclusion that many more Lorentzians now contribute to the overall noise spectrum.

The exact shape of the band bending must be known and the Langevin sources for the position-dependent transport equations must be given. The spectra can then be computed with Green's function methods (see Van Vliet and Mehta[38] or with the transfer impedance method).[39] This requires a separate study and is outside the scope of this article. We still note that similar problems were encountered in noise studies in amorphous silicon by Verleg and Dijkhuis;[40] in particular, Sec. V D.

VI. DISCUSSION OF RESULTS AND CONCLUSIONS

For device ND-101, the time constants are given in Tables I and II and the Arrhenius plots in Fig. 8. Employing the exponential relationship Eq. (27) for the trap depth $\varepsilon_C - \varepsilon_i$ (distance below the conduction band), we obtained the trap energies of Table III. Likewise, for ND-102 (for which less data were obtained) the likely trap depths are given also in Table III. Altogether, there is a reasonable similarity for the trapping energies in the two devices. The deepest traps are ~660 meV, while the shallowest traps have an energy of ~190 meV. These values are roughly twice those observed in $Al_xGa_{1-x}As$/GaAs MODFETs by Yuping Chen.[1] Since the band gap is much larger in nitride-based MODFETs, this overall result is quite acceptable. The deep traps must occur where the band distance $\varepsilon_C - \varepsilon_F$ is largest, i.e., near the interface; also, we expect that these traps are abundant and possibly well below the Fermi level. The shallower traps are more prevalent in the measured spectra, having corner frequencies in the kHz to MHz range. These traps are showing up further away from the interface, but are probably present throughout the $Al_xGa_{1-x}N$ layer. We also give in Table III, trap-level energies obtained in GaN by the deep level transient spectroscopy (DLTS) technique.

TABLE III. Trap energies in GaN. Columns 1 and 2 report values obtained in this work, corresponding to sample ND-101 and ND-102. Column 3 reports trap energies observed experimentally by other workers.

ND-101 (meV)	ND-102 (meV)	DLTS (meV)[a]
659	661	670[b]
543	⋯	600[c]
482	485	450[c]
438	438	⋯
370	⋯	⋯
301	294	300[c]
270	⋯	270[d]
243	249	250[c]
191	191	200[e]

[a]DLTS stands for deep level transient spectroscopy, a technique capable of determining electron and hole trap parameters. For details see Ref. 41.
[b]Reference 42.
[c]Reference 43.
[d]Reference 44.
[e]Reference 45.

Auret and Goodman[46] obtained trap depths by plotting $\log(T^2/e)$ versus $1000/T$, where e is the emissivity as defined in this spectroscopic method (see Refs. 17, 28, and 47). It is to be noted that their e corresponds to our $1/\tau$, Eq. (27). Their Arrhenius plot is given in Ref. 46, Fig. 1. The similarity with our figures (see Fig. 8), obtained from noise data, is striking. Note, however, that the noise measurements reveal much lower τ values (down to $\sim 10^{-7}$ s) whereas DLTS data typically go down only to $\tau \sim 1$ ms.

In conclusion, we attribute the Lorentzian noise of our devices to a large range of traps present in the $Al_xGa_{1-x}N$ layer, adjacent to the interface with GaN. The $1/f$-like noise is quite low at all temperatures and probably stems from defect states associated with the internal source and/or drain contacts. The noise could probably be reduced by perfecting the deposition techniques.

ACKNOWLEDGMENTS

This work has been supported by a grant to the Future Aerospace Science and Technology (FAST) Center at FIU

from the Air Force Office of Scientific Research (AFOSR) under Contract No. F49620-00-1-0379. The authors thank Dr. Yun of Virginia Commonwealth University for providing them with the devices reported on in this article.

[1] Y. Chen, C. M. Van Vliet, G. L. Larkins, Jr., and H. Morkoç, IEEE Trans. Electron Devices **47**, 2045 (2000).
[2] Y. Chen, C. M. Van Vliet, P. M. Koenraad, and G. L. Larkins, Jr., J. Appl. Phys. **86**, 6206 (1999).
[3] Fourth International Conference on Nitride Semiconductors, Denver, CO; Phys. Status Solidi B **228** (2001).
[4] L. Eastman and U. K. Mishra, IEEE Spectrum **39**(5), 28 (2002).
[5] H. Morkoç, S. Strite, G. B. Gao, M. E. Lin, B. Sverdlov, and M. Burns, J. Appl. Phys. **76**, 1363 (1994).
[6] S. C. Binari and H. C. Dietrich, in *GaN and Related Materials*, edited by S. J. Pearton (Gordon and Breach, New York, 1997), pp. 509–534.
[7] S. Strite and H. Morkoç, J. Vac. Sci. Technol. B **10**, 1237 (1992).
[8] J. C. Tan, J. S. Williams, J. Zou, D. J. H. Cockayne, S. J. Pearton, and J. C. Zoppler, Appl. Phys. Lett. **72**, 1190 (1998).
[9] J. C. Zoppler *et al.*, J. Electron. Mater. **27**, 179 (1998).
[10] X. A. Cao *et al.*, Appl. Phys. Lett. **73**, 229 (1998).
[11] J. D. Albrecht, R. P. Wang, P. P. Ruden, M. Farahmand, and K. F. Brennan, J. Appl. Phys. **83**, 4777 (1996).
[12] B. Gelmont, K. Kim, and M. Shur, J. Appl. Phys. **74**, 1818 (1993).
[13] S. C. Jain, M. Willander, J. Narayan, and R. Van Overstraeten, J. Appl. Phys. **87**, 965 (2000).
[14] A. Rizzi, in *6H-SiC(0001)/AlN/GaN Epitaxial Heterojunctions and Their Valence Band Offsets*, Nato ASI Series, Heterostructure Epitaxy and Devices, edited by Peter Korols (NATO, 1995).
[15] J. Wagner, H. Obloh, M. Kunzer, M. Maier, and K. Köhler, J. Appl. Phys. **89**, 2779 (2001).
[16] U. Tisch, B. Meyler, O. Katz, E. Finkman, and J. Salzman, J. Appl. Phys. **89**, 2676 (2001).
[17] M. Shur, *GaAs Devices and Circuits* (Plenum, New York, 1987).
[18] G. Zorpette, IEEE Spectrum **39**(6), 18 (2002).
[19] J. A. Garrido, F. Calle, E. Muñóz, I. Izpura, J. L. Sánchez-Rojas, and R. Li, K. L. Wang, AIP Conf. Proc. **466**, 71 (1998).
[20] A. A. Balandin, *Proceedings of the 16th International Conference on Noise in Physical Systems and* 1/*f Fluctuations (ICNF)*, edited by G. Bosman (World Scientific, Singapore, 2001), p. 227.
[21] S. L. Rumyantsev, M. E. Levinshtein, R. Gaska, M. S. Shur, A. Khan, J. W. Wang, G. Simion, A. Ding, and T. Adesida, Phys. Status Solidi A **176**, 201 (1999).
[22] S. L. Rumyantsev, N. Pala, M. S. Shur, R. Gaska, M. L. Levinshtein, M. Asif Khan, G. Simin, X. Hu, and J. Yang, J. Appl. Phys. **88**, 6726 (2000).
[23] B. H. Leung, W. K. Fong, C. F. Zhu, and C. Surya, J. Appl. Phys. **91**, 3706 (2002).
[24] M. E. Levinshtein, S. L. Rumyantsev, D. C. Look, R. J. Molnar, M. Asif Khan, G. Simin, V. Adivarahan, and M. S. Shur, J. Appl. Phys. **86**, 5075 (1999).
[25] S. L. Rumyantsev, N. Pala, M. S. Shur, R. Gaska, M. L. Levinshtein, M. Asif Khan, G. Simin, X. Hu, and J. Yang, J. Appl. Phys. **90**, 310 (2001).
[26] R. S. Duran, G. L. Larkins, Jr., C. M. Van Vliet, and H. Morkoç, 9th van der Ziel Symposium on Quantum 1/f Noise and other Low Frequency Phenomena, Richmond, VA, August 1–2, 2002.
[27] M. A. Reshchikov, D. Visconti, and H. Morkoç, Appl. Phys. Lett. **78**, 177 (2001).
[28] A. van der Ziel, *Noise: Sources, Characterization, and Measurement* (Prentice Hall, Englewood Cliffs, N.J., 1970).
[29] B. R. Nag, *Theory of Electrical Transport in Semiconductors* (Pergamon, Oxford, 1972).
[30] N. Paul, C. M. Van Vliet, and S. Mergui, J. Appl. Phys. **85**, 8287 (1999).
[31] Even small shifts of the Lorentzians horizontally or vertically produced a noticeable disagreement with the envelope spectrum.
[32] C. M. Van Vliet, in *Proceedings of the 16th International Conference on Noise in Physical Systems and* 1/*f Fluctuations (ICNF)*, edited by G. Bosman (World Scientific, Singapore, 2001), p. 561.
[33] C. M. Van Vliet, J. Appl. Phys. (in press).
[34] A. D. Van Rheenen, G. Bosman, and R. J. J. Zijlstra, Solid-State Electron. **30**, 259 (1987).
[35] J. A. Copeland, IEEE Trans. Electron Devices **18**, 50 (1971).
[36] C. M. Van Vliet, IEEE Trans. Electron Devices **41**, 1902 (1994).
[37] K. M. Van Vliet and J. R. Fassett. in *Fluctuation Phenomena in Solids*, edited by R. E. Burgess (Academic, New York, 1965), pp. 267–354.
[38] C. M. Van Vliet and H. Mehta, Phys. Status Solidi B **106**, 11 (1981).
[39] K. M. Van Vliet, A. Friedmann, R. J. J. Zijlstra, A. Gisolf, and A. van der Ziel, J. Appl. Phys. **46**, 1804 (1975).
[40] P. A. W. E. Verleg and J. I. Dijkhuis, Phys. Rev. B **58**, 3904 (1998).
[41] D. C. Look, Phys. Status Solidi B **228**, 293 (2001).
[42] D. Haase, M. Schmid, W. Kürner, A. Dörnen, V. Härle, F. Scholz, M. Burkard, and H. Schweizer, Appl. Phys. Lett. **69**, 2525 (1996).
[43] A. Y. Poliakov, A. S. Usikov, Bl Theys, N. B. Smirnov, A. V. Govorkov, F. Jomard, N. M. Shmidt, and W. V. Lundin, Solid-State Electron. **44**, 1971 (2000).
[44] S. A. Goodman, F. D. Auret, M. J. Legodi, B. Beaumont, and P. Gibart, Appl. Phys. Lett. **78**, 3815 (2001).
[45] F. D. Auret, W. E. Meyer, S. A. Goodman, F. K. Loschnick, J. M. Spaeth, B. Beaumont, and P. Gibart, Physica B **273/274**, 92 (1999).
[46] F. D. Auret and S. A. Goodman, in *III-Nitride Semiconductors: Electrical, Structural and Defects Properties*, edited by O. Manasreh (Elsevier Science B. V., Amsterdam, 2000), p. 251.
[47] Shur's formula is incorrect; the trap degeneracy factor g [Eq. (3-7-21)] should be in the numerator.